Electrothermal free-form additive manufacturing of thermosets

Anubhav Sarmah[a,†], Ethan M. Harkin[a,†], Thang Q. Tran[a,b], Matthew J. Cupich[a], Micah J. Green[a,c]*

[a] Artie McFerrin Department of Chemical Engineering, Texas A&M University, College Station, TX, 77843, USA

[b] Singapore Institute of Manufacturing Technology (SIMTech), Agency for Science, Technology and Research (A*STAR), 2 Fusionopolis Way, Singapore 138634, Singapore

[c] Department of Materials Science & Engineering, Texas A&M University, College Station, TX, 77843, USA

[†:] These authors contributed equally to the work.

* Corresponding author: E-mail: micah.green@tamu.edu (Micah J. Green)

Abstract

Despite the extensive use of thermosetting resins, additive manufacturing of such materials is limited. Traditional processing requires either (i) long curing schedules to avoid the collapse of an uncured printed part or (ii) changes to the resin chemistry and curing mechanism. This work demonstrates a material-extrusion based setup capable of printing and curing any industry-standard thermoset resin through the use of electric fields and carbon nanomaterial susceptors. A material extrusion printer is used to deposit the liquid ink, composed of uncured epoxy with a carbon nanotube filler. After each layer is deposited, the nanotube-loaded ink is exposed to radio frequency (RF) fields generated by a coaxial applicator suspended over the part. The resulting current generates heat rapidly and volumetrically, curing the resin, preventing part collapse, and enabling further printing. This methodology enables rapid additive manufacturing of arbitrarily large structures with low viscosity resins that are otherwise impossible to print.

Keywords: Additive manufacturing, material extrusion, radio-frequency fields, electrothermal, epoxy nanocomposite

1. Introduction

Thermosets are polymeric materials that crosslink when heated and cured and have widespread applications in fields such as aerospace engineering, automobile engineering, and structural energy storage.[1-3] Additive manufacturing of thermosets has received growing attention over the last few years since this technology would allow for custom part manufacturing, free-form fabrication, and eliminate the dependence on molds.[4-6]

Direct ink writing (DIW) is a material extrusion based printing method applicable to thermoset additive manufacturing.[7,8] In this process, the resin 'ink' is deposited along digitally designed paths, extruded at a controlled rate. However, additive manufacturing of thermosets using DIW comes with a unique set of challenges: Firstly, the printed part tends to buckle under its own load as the yield stress of the uncured resin ink is exceeded.[9-13] Thermosets require curing at elevated temperatures for better crosslinking and enhanced final part properties, such as glass transition temperature, tensile strength, and elastic modulus.[14,15] Additionally, the uncured printed part can also collapse while curing in a thermal oven; as the uncured epoxy begins to heat up, the viscoelastic fluid undergoes a drop in viscosity (and a collapse) before the curing reaction begins.[16-18]

One approach to allow for 3D printing of crosslinkable resins is the use of rapid *in situ* curing; this can be accomplished using photocurable polymers, dual-cure resins (photopolymers mixed with a thermoset), or fast-curing resins.[19-23] However, these approaches are all restricted to certain resin formulations, most of which have limited industrial applications. These challenges pose a fundamental scientific question of how conventional thermosets can be 3D printed without alterations to their chemistry.

Instead of *in situ* curing, the most common solution to print conventional resins is to load the uncured resin ink with viscosity-modifying agents.[13,24-26] These fillers increase the yield stress of the ink, allowing for shape retention while printing tall structures without changing resin chemistry. However, this approach can have several drawbacks. Excessive addition of fillers makes a uniform dispersion difficult to attain, often embrittling the final part.[27-29] Also, such printing approaches are usually followed by a long curing schedule (~24 hours) at relatively low temperatures in order to avoid collapse as described above, thus significantly increasing the total processing time of the part.[16,30]

We hypothesize that the use of *in situ* thermal curing will expand both the range of printable chemistries and the processing parameter space for printing these resins. By partially curing each printed layer before subsequent layers are added, the yield strength of the part is increased and the problems of buckling under self-weight and collapse during curing are avoided. This approach requires on-demand, local heating of the part being printed. One such technique to induce rapid, localized heating is radio-frequency (RF) heating.[31,32] RF fields interact with carbon materials to generate electrothermal heating, granting extreme heating rates in a localized area.[33-39] By loading epoxy resin with carbon nanotubes (CNTs), the resin becomes electrically conductive, and heat up when exposed to RF fields.[40-45] Our group has previously demonstrated proof-of-concept of this technology for material extrusion printing with RF fields.[46]

This paper demonstrates a new unified device which couples a DIW printer and an RF applicator for the printing of CNT-loaded epoxy resins via a cyclic printing and curing process (**Figure 1**). First, a layer of uncured ink <1 mm thick is deposited. After the layer is fully printed, the printing bed is positioned below an onboard, suspended applicator (**Figure S1**); a fringing, out-of-plane electric field is generated by the coplanar RF applicator. This allows for localized heating and curing of the exposed resin. The RF field only penetrates through approximately the uppermost 5 mm of the part. This means only recently deposited layers receive significant heating. This targeted heating initiates curing of the top layer, increases the ink yield strength, and prepares the part for continued printing, all while simultaneously leaving fully cured layers lower in the printed structure alone. After partial curing via RF is complete, printing resumes and the cycle repeats. This technology enables the printing of thermosets of arbitrarily large sizes, allowing for rapid additive manufacturing of mechanically strong nanocomposite parts.

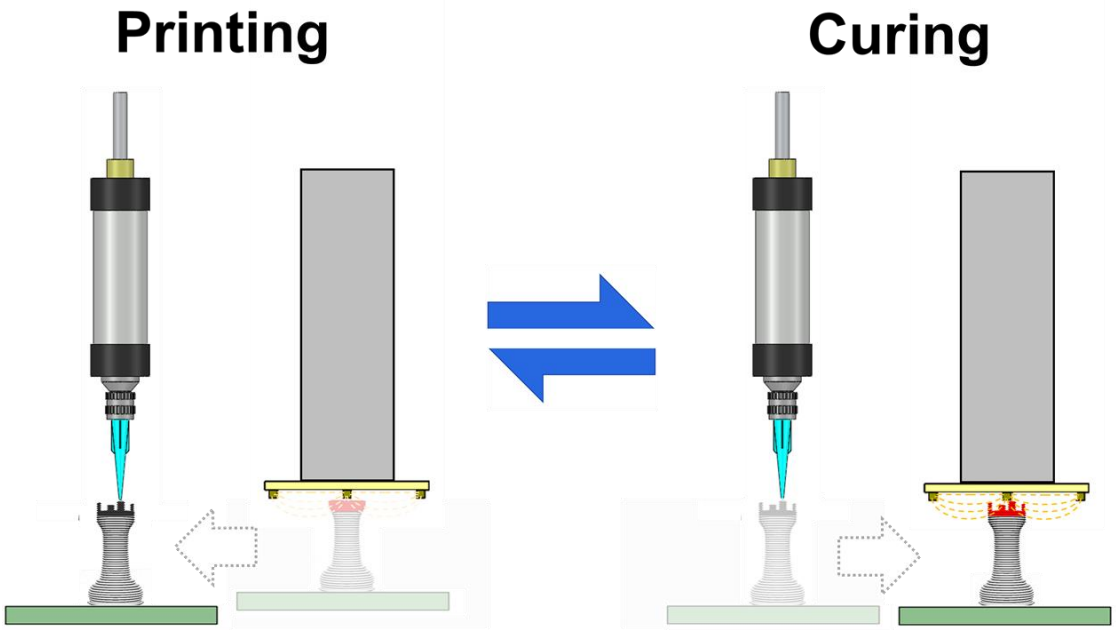

Figure 1: Schematic showing integrated Direct Ink Writing (DIW) and Radio-frequency (RF) Heating setup. The DIW nozzle pauses after depositing every layer of uncured resin on the printbed; the printbed moves in the x-y plane to position itself under an RF applicator which generates a fringing field in the downward direction. The resin locally heats and partially cures when exposed to RF fields; the printbed re-positions itself under the nozzle to resume the print, and the entire process is repeated.

2. **Materials and Methods**

2.1 Materials: EPON 828, a bi-functional Bisphenol-A derived epoxide supplied by Hexion (Columbus, OH) and Jeffamine T403, a tri-functional primary amine supplied by Huntsman Corp (The Woodlands, TX) were mixed in a 1:0.49 ratio by weight to make the resin used for all experiments. Multi-walled carbon nanotubes (MWCNTs) supplied by Cheaptubes (Cambridgeport, VT) were added to the resin and mixed using a planetary mixer, at various loadings between 1 and 13% for the rheological tests. For printing experiments, a loading of 10 wt.% was used.

2.2 Rheology: Rheological measurements were carried out using a parallel-plate fixture in a stress-controlled rheometer (Anton Paar, MCR 301) at room temperature with a 25 mm diameter stainless steel top fixture and a 50 mm disposable aluminum plate bottom fixture with a gap of 0.1 mm. To determine the low-shear viscosity of resins, the sample was subjected to a constant shear rate of 0.01 s^{-1}, and viscosity as a function of time was measured. To evaluate the yield stress of resins, an oscillatory amplitude sweep was run at 1 Hz.

2.3 Degree of Cure calculation: The degree of cure as a function of curing temperature and time was determined by numerically solving the kinetic model shown in **Equation 2**. The values of the constants used to solve this model are given in **Table S1**.[18]

2.4 Coupled Direct Ink Writing (DIW) and Radio-Frequency (RF) Heating setup: The HyRel (Hyrel 3D; Norcross, GA) Engine Standard Resolution (Engine SR) direct ink writing printer was used for printing experiments. The resin ink was loaded into a 15-cc dual-gasket stainless steel cartridge for a HyRel EMO-XT print head, and a nozzle of width 0.84 mm (Structur3D) was attached to the print head. The CAD files of structures to be printed were created using Solidworks and converted into g-codes using Hyrel's Repetrel software along with Slic3r.

To generate the RF fields, a coplanar applicator (fabricated by laser-etching copper traces on an FR4 substrate) was suspended upside down over the printbed, such that the printed layers were exposed to RF fields from the top. RF waves were generated using a RIGOL DSG15 signal generator and amplified using a PRANA GN 500 amplifier. The RF waves were supplied to the applicator using a coaxial cable. The RF fields had a frequency of 168 MHz, and the power was modulated by hand such that the top layer was maintained at ~75 °C for 10 minutes. The temperature of the sample was monitored using a FLIR A500 thermal camera.

2.5 Optical Microscopy: Optical microscopy images were captured using an Olympus BX51 microscope.

3. Results and Discussion

3.1 Rheology and Curing Rate: Before printing, we analyze the rheological behavior of the ink itself as a function of filler loading. We determined the zero-shear viscosity of the CNT-loaded resin (at different filler loadings) using rheological measurements (**Figure 2a**). Next, we performed a stress sweep test of the CNT-loaded resin (**Figure S2**) to determine the yield stress of the CNT-loaded resin at various filler loadings (**Figure 2b**). As expected, the zero-shear viscosity and yield stress of the resin increased with increase in filler loading. Resin thixotropy was investigated in prior work, with loadings above 4% showing acceptable recovery after shear.[44]

The kinetics of the curing reaction are well-understood from our prior work. Curing rate is the reciprocal of the time required for the resin to reach 95% cure and is controlled by process temperature; this means that higher curing rates indicate shorter curing times and higher processing temperatures (**Figure S3**).[18,43]

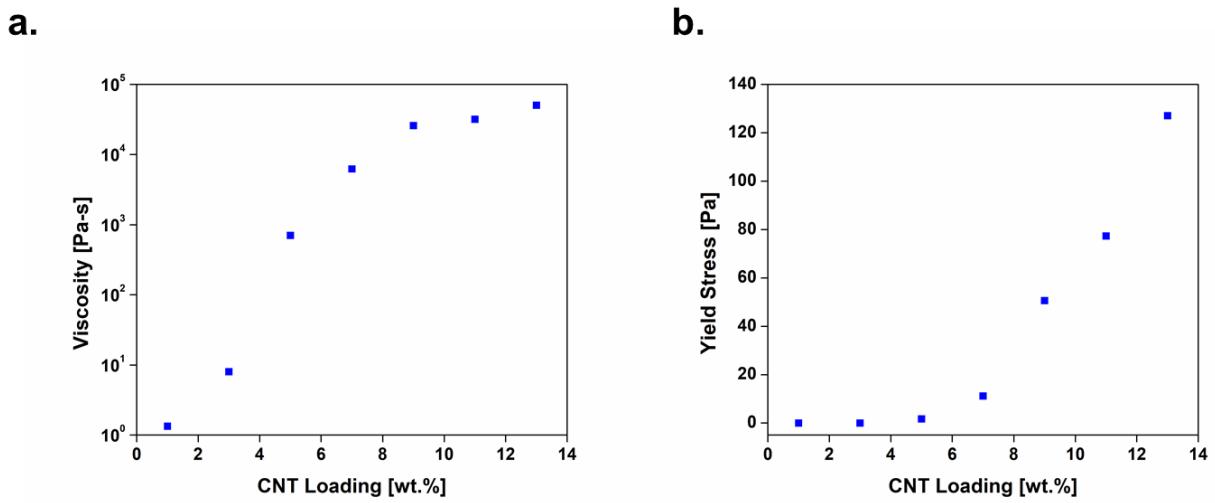

Figure 2: (a) Viscosity at room temperature measured at shear rate = 0.001 s^{-1} for uncured resin at different CNT loadings. (b) Yield stress at room temperature for uncured resin at different CNT loadings.

3.2 DIW printability mapping: We determine how RF fields can widen the range of resin compositions that can be successfully printed using DIW. **Figures 3a and 3b** show parameter space maps for DIW printing, where the yield stress of the ink (based on composition and filler loading) is listed on the x-axis and the curing rate (based on curing temperature) is shown on the y-axis. **Figure 3a** corresponds to conventional DIW while **Figure 3b** corresponds to our new method, discussed in more detail below. The map is divided into regions that indicate different outcomes for the print, showing whether a given print process will be successful or not. The red region denotes printing conditions where the part collapses because it is unable to support its own weight (low yield stress). The yellow region shows cases where printing was successful, but post-curing at a given temperature causes collapse. A successful print-and-cure process is indicated in the green region. For our test printed geometry, we selected printed walls with a width of 0.8 mm, layer height of 0.2 mm, and total height of 0.6 mm. We then experimentally printed these test walls

with and without RF heating, with inks of varying CNT loading and varying cure temperatures (post-printing) and assessed whether these walls would hold their shape. (Additional representative images of printing for all the different zones are shown in the margins of **Figure 3**.)

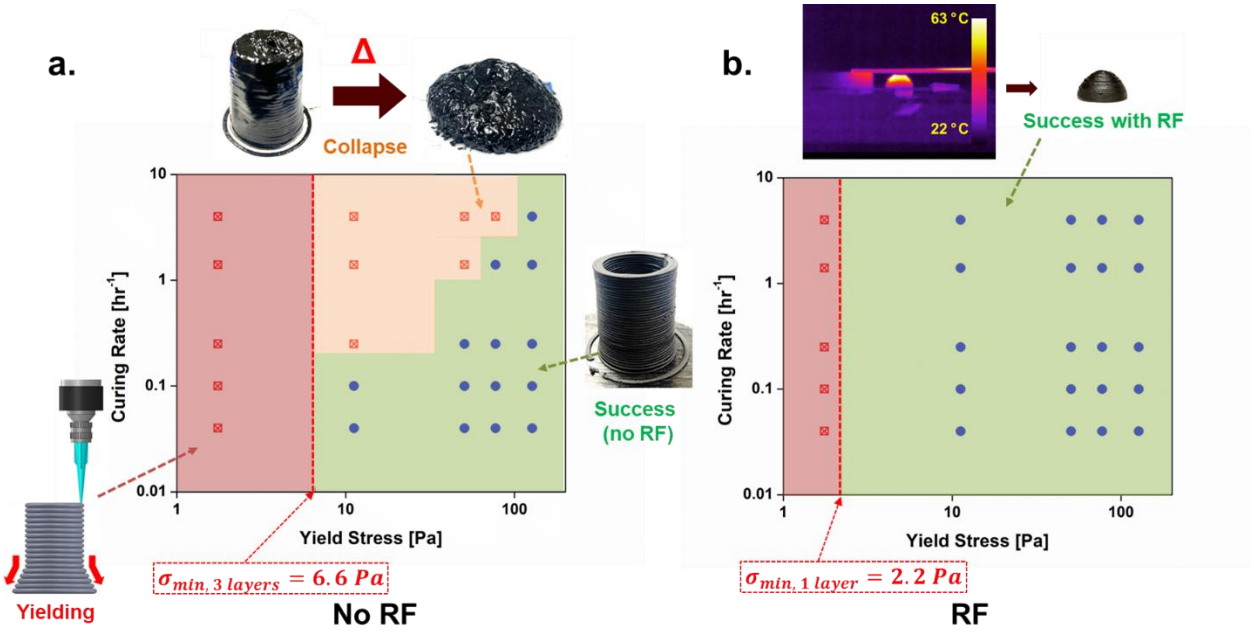

Figure 3: Parameter space of printing for a three-layered, single-trace wall of thermoset resins via DIW with varying yield stress values (depending on CNT loading) at different curing rates (depending on curing temperatures). CNT loadings tested here are: 5, 7, 9, 11, and 13 wt.%. Red markers depict a failed print, blue markers represent successful prints. The red zone depicts collapse during printing, and its boundary is dictated by Equation 1; yellow zone depicts collapse during curing; and the green zone depicts successful printing and curing for: (a) DIW with conventional curing, and (b) RF-assisted DIW. Representative images for each zone denoted by dotted arrows.

We first analyze the limits of conventional DIW (**Figure 3a**), which involves extruding liquid material layer by layer, then curing and solidifying the printed part in a convective oven. For extremely low yield stress fluids (shown in red zone), the wall will collapse during the printing process itself, making such loadings near-impossible to print. The relation between minimum yield stress (σ_{min}) for a given part height (h) can be given as

$$\sigma_{min} = \rho g h \qquad (1)$$

where ρ is density of printed material and g is acceleration due to gravity.[10] For the geometry we are testing, a minimum yield stress of ~6-7 Pa is needed for the 3-layer wall to avoid collapse under its own load; this is represented by the right edge of the red zone. As the yield stress increases, the resin becomes printable, provided a slow curing rate is maintained (associated with a low curing temperature). If the curing rate is too high, the printed part will collapse in the oven because of reduction of resin viscosity at high temperatures (yellow zone). Given a high filler loading or a very slow curing rate, the resin will be stable enough for the printed part to hold its shape throughout the entire process (green zone).

The parameter space for RF-assisted DIW printing is shown in **Figure 3b**. As expected, the minimum safe printable ink modulus (depicted by the right edge of the red zone) is lower in the RF-assisted process (~2-3 Pa). This is because RF fields allow for *in situ* heating and partial curing of each deposited layer. This enables the bottom layers to bear load when subsequent top layers are printed, thereby eliminating the possibility of collapse. RF-assisted printing eliminates the yellow zone because there is no post-cure process needed, thus allowing for rapid manufacturing of resins with lower CNT loadings.

3.3 Variation of degree of cure with z-height: We next analyze how RF fields affect the degree of cure achieved by the part during the print itself. (For subsequent printing experiments, 10 wt.% CNT-loaded resin was used.) As described previously, RF fields were applied from above for every printed layer. For a DIW-printed wall, the RF input power was modulated such that the top surface of each deposited layer was maintained at ~70-75 °C for ~10 minutes, monitored using a FLIR A500 thermal camera (**Figure S4**). We determined the temperature distribution as a function of depth when exposed to RF fields (**Figure 4a**). Due to the applicator's location above the printed part and the limited range of the chosen RF applicator (~1-2 mm), we observed a drop in temperature with increasing distance from the top, which can be clearly seen from the surface plot of the temperature distribution (**Figure 4c**). However, the temperature distribution plots for different layers overlap with one another, thus proving that RF fields can successfully heat the top surface irrespective of the total part height.

Next, we determined the corresponding degree of cure for each printed layer (**Figure 4b**) maintained at the temperatures shown in **Figure 4a**. The degree of cure (α) for this resin as a function of temperature can be given as

$$\frac{d\alpha}{dt} = (k\alpha^m)(1-\alpha)^n \quad (2)$$

where *k* is the temperature dependent reaction rate constant, and *m* and *n* are empirical reaction constants. The values of all constants used to solve this model are given in **Table S1** and were experimentally determined in our prior work.[18] **Figure 4d** shows a surface plot of the degree of cure distribution for the printed part after being exposed to *in situ* RF heating. The first layer reached a degree of cure value of ~0.55 at the end of the first heating pass. After the second layer was deposited, the fresh layer at the top again reached a degree of cure of ~0.55, while the partially cured first layer further cured to reach ~0.83 conversion. By the end of the fourth heating pass, the first layer was almost completely cured (~0.97). This print-and-cure schedule increases the mechanical integrity of the deposited layers and also allows for interlayer adhesion between the printed layers.

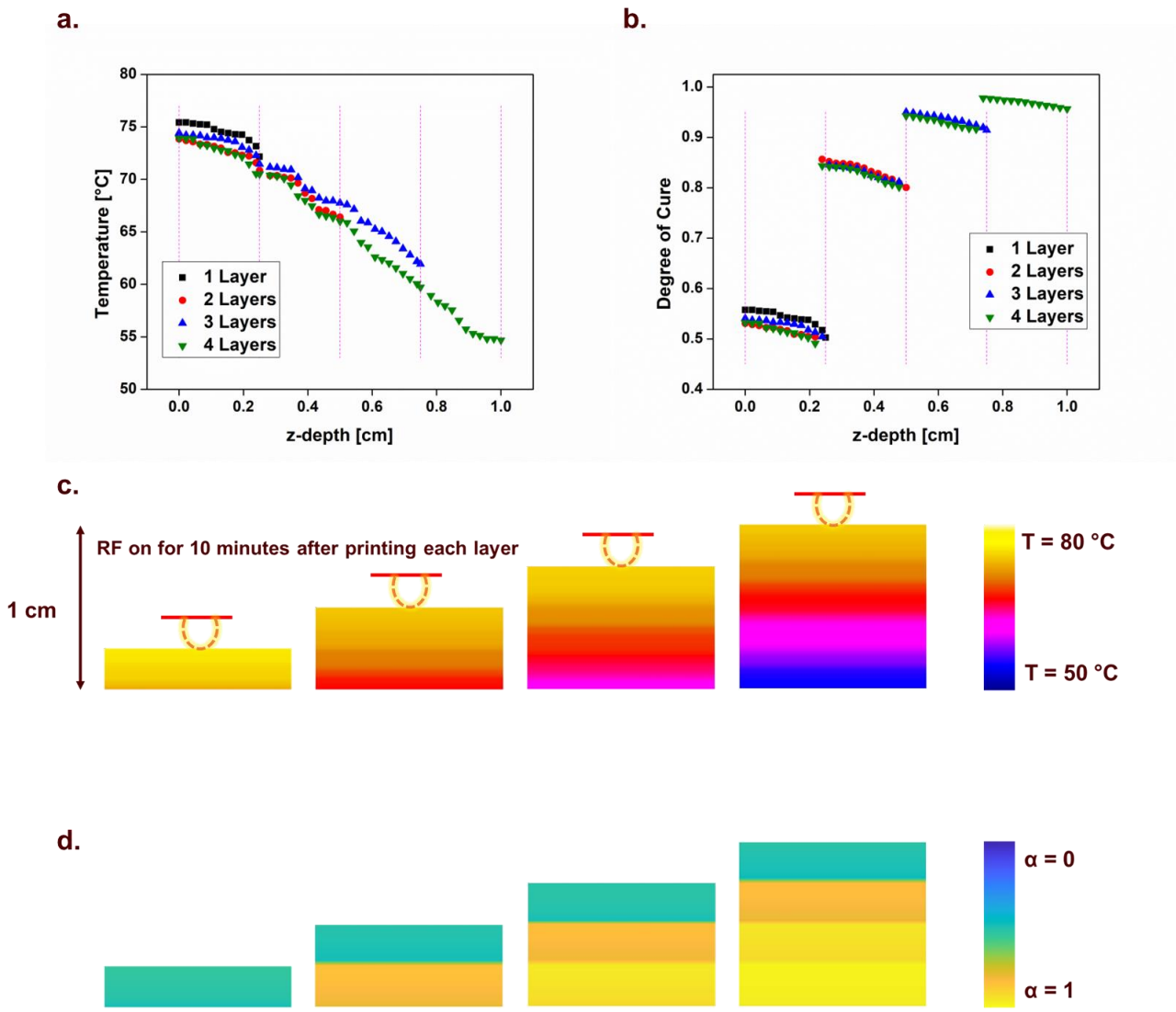

Figure 4: (a) Maximum temperature vs. z-depth measured using a FLIR thermal camera for a 4-layered print (each layer = 0.25 cm). Deposited layers were exposed to RF such that the top surface is maintained at ~75 °C for 10 minutes. (b) Degree of cure vs. z-depth calculated based on temperature distribution shown in Figure 4a. (c) Surface plot of temperature variation across z-height measured using a FLIR camera for a DIW-printed wall. (d) Surface plot of degree of cure calculated as a function of z-height based on thermal data shown in Figure 4a.

3.4 Additive Manufacturing using RF-assisted DIW: To demonstrate the utility of this method, 3D shapes including hollow cylinders and hemispherical domes were printed both via conventional DIW (no *in situ* curing), and our coupled DIW-RF methodology (print-and-cure cycle after every few layers). As shown in **Figure 5a**, the conventionally printed samples collapsed after a few layers. This was expected because the part was unable to sustain itself once the weight of the part went beyond the yield stress of the uncured resin. However, for samples exposed to RF fields between printed layers, the bottom layers were able to heat (observed using a thermal camera) and cure before depositing the top layers, thus enabling the printed part to maintain resolution. We

further demonstrate the applicability of the coupled DIW-RF methodology for additive manufacturing of tall, complex shapes by printing a vase and a rook chess piece (**Figure 5b**). Optical microscopy was conducted on the surface of the cylinder printed using RF-assisted DIW (**Figure 5a**); as shown in **Figure 5c**, the individual layers did not sag or lose resolution. In our previous work, we have also shown how volumetric RF heating can enhance the mechanical properties of a part compared to a conventional, oven-cured part (**Figure S5**), thus establishing RF heating as a promising route for rapid manufacturing of thermoset composites with superior mechanical properties.[46]

Figure 5: (a) Direct Ink Writing of epoxy parts with and without *in situ* exposure to RF fields. When RF fields are applied from above to heat and cure the part before the subsequent layer is deposited, the structure is printed successfully without loss of resolution. However, if the layers are not cured while printing, the part collapses under its own load, leading to a failed print. (b) Chess rook and flower vase printed using RF-assisted DIW printing. (c) Optical microscopy of DIW-printed part with *in situ* curing between each layer (scale bar is 100 μm).

4. Conclusions

The results of this work describe a unified device that successfully couples a radio-frequency applicator with a commercial direct ink writing printer to enable the additive manufacturing of conventional thermosets. Radio-frequency fields broaden the range of resin yield stress values (determined by filler loading) that can be printed via DIW, thus allowing for additive manufacturing of relatively low viscosity resins and eliminating the requirement of viscosity-modifying agents. We attempted the printing of tall, complex shapes via both conventional DIW and DIW coupled with RF heating after each layer; as expected, the sample printed using conventional DIW collapsed beyond a few layers, while the part printed using our coupled methodology was able to maintain its shape and resolution. *In situ* RF heating opens a doorway to

rapid processing of thermosets, thus significantly reducing the long curing schedules usually associated with additive manufacturing of such materials. The unified device described here allows for rapid, free-form fabrication of conventional thermosets with no additional post-curing, thus addressing one of the longstanding problems associated with this field.

Acknowledgements

The authors acknowledge A*STAR Graduate Academy – A*STAR International Fellowship Program for their sponsorship. This work was supported by Honeywell Federal Manufacturing & Technologies, LLC, which operates the Kansas City National Security Campus for the United States Department of Energy/National Nuclear Security Administration under Contract Number DE-NA0002839.

Author Contributions

A.S. and E.M.H. contributed equally to this work. A.S. and E.M.H. conceived the idea and designed the experiments. T.Q.T. and M.J.C. assisted with experiments. A.S. and E.M.H. collectively wrote the paper. M.J.G. provided technical supervision and review.

Conflict of Interest

The authors declare no conflict of interest.

References

1. Q. Guo. *Thermosets: structure, properties, and applications.* Woodhead Publishing; 2017.
2. B. Bilyeu, W. Brostow, K. P. Menard. Epoxy thermosets and their applications I: chemical structures and applications. *Journal of Materials Education.* **1999**;21(5/6):281-286.
3. W. Johannisson, D. Zenkert, G. Lindbergh. Model of a structural battery and its potential for system level mass savings. *Multifunctional Materials.* **2019**;2(3):035002.
4. M. Peerzada, S. Abbasi, K. T. Lau, N. Hameed. Additive manufacturing of epoxy resins: Materials, methods, and latest trends. *Industrial & Engineering Chemistry Research.* **2020**;59(14):6375-6390.
5. M. B. A. Tamez, I. Taha. A review of additive manufacturing technologies and markets for thermosetting resins and their potential for carbon fiber integration. *Additive Manufacturing.* **2021**;37:101748.
6. A. G. Crowley, T. Q. Tran, M. J. Green. Using nanomaterials to enhance the additive manufacturing of polymeric resins. *Nano Futures.* **2022**;6(4):042502.
7. J. A. Lewis. Direct ink writing of 3D functional materials. *Advanced Functional Materials.* **2006**;16(17):2193-2204.
8. M. Saadi, A. Maguire, N. T. Pottackal, M. S. H. Thakur, M. M. Ikram, A. J. Hart, P. M. Ajayan, M. M. Rahman. Direct ink writing: a 3D printing technology for diverse materials. *Advanced Materials.* **2022**;34(28):2108855.
9. J. K. Wilt, D. Gilmer, S. Kim, B. G. Compton, T. Saito. Direct ink writing techniques for in situ gelation and solidification. *MRS Communications.* **2021**;11:106-121.
10. A. M'barki, L. Bocquet, A. Stevenson. Linking rheology and printability for dense and strong ceramics by direct ink writing. *Scientific reports.* **2017**;7(1):6017.
11. Y. Eom, F. Kim, S. E. Yang, J. S. Son, H. G. Chae. Rheological design of 3D printable all-inorganic inks using BiSbTe-based thermoelectric materials. *Journal of Rheology.* **2019**;63(2):291-304.
12. S. K. Romberg, A. P. Kotula. Simultaneous rheology and cure kinetics dictate thermal post-curing of thermoset composite resins for material extrusion. *Additive Manufacturing.* **2023**;71:103589.
13. S. K. Romberg, M. A. Islam, C. J. Hershey, M. DeVinney, C. E. Duty, V. Kunc, B. G. Compton. Linking thermoset ink rheology to the stability of 3D-printed structures. *Addit Manuf.* **2021**;37.
14. R. Carbas, E. Marques, L. Da Silva, A. Lopes. Effect of cure temperature on the glass transition temperature and mechanical properties of epoxy adhesives. *The Journal of Adhesion.* **2014**;90(1):104-119.
15. A. S. Ismail, M. Jawaid, N. H. Hamid, R. Yahaya, A. Hassan, M. Asim, A. Supian. Effect of curing temperature on mechanical properties of bio-phenolic/epoxy polymer blends. *Journal of Polymers and the Environment.* **2021**:1-8.
16. M. G. Wimmer, B. G. Compton. Semi-solid epoxy feedstocks with high glass transition temperature for material extrusion additive manufacturing. *Additive Manufacturing.* **2022**;54:102725.
17. Q. Chen, L. Han, J. Ren, L. Rong, P. Cao, R. C. Advincula. 4D printing via an unconventional fused deposition modeling route to high-performance thermosets. *ACS applied materials & interfaces.* **2020**;12(44):50052-50060.
18. G. B. Tezel, A. Sarmah, S. Desai, A. Vashisth, M. J. Green. Kinetics of carbon nanotube-loaded epoxy curing: Rheometry, differential scanning calorimetry, and radio frequency heating. *Carbon.* **2021**;175:1-10.
19. T. Wu, P. Jiang, X. Zhang, Y. Guo, Z. Ji, X. Jia, X. Wang, F. Zhou, W. Liu. Additively manufacturing high-performance bismaleimide architectures with ultraviolet-assisted direct ink writing. *Materials & Design.* **2019**;180:107947.
20. S. K. Romberg, C. J. Hershey, J. M. Lindahl, W. G. Carter, J. Condon, V. Kunc, B. G. Compton. Large-scale reactive thermoset printing: Complex interactions between temperature evolution, viscosity, and cure shrinkage. *The International Journal of Advanced Manufacturing Technology.* **2022**;123(9-10):3079-3094.

21. L. Wei, J. Li, S. Zhang, B. Li, Y. Liu, F. Wang, S. Dong. Fabrication of SiOC ceramic with cellular structure via UV-Assisted direct ink writing. *Ceramics International.* **2020**;46(3):3637-3643.
22. R. Tu, H. A. Sodano. Additive manufacturing of high-performance vinyl ester resin via direct ink writing with UV-thermal dual curing. *Additive Manufacturing.* **2021**;46:102180.
23. I. Binyamin, E. Grossman, M. Gorodnitsky, D. Kam, S. Magdassi. 3D Printing Thermally Stable High-Performance Polymers Based on a Dual Curing Mechanism. *Advanced Functional Materials.* **2023**:2214368.
24. N. S. Hmeidat, D. S. Elkins, H. R. Peter, V. Kumar, B. G. Compton. Processing and mechanical characterization of short carbon fiber-reinforced epoxy composites for material extrusion additive manufacturing. *Composites Part B: Engineering.* **2021**;223:109122.
25. B. G. Compton, J. K. Wilt, J. W. Kemp, N. S. Hmeidat, S. R. Maness, M. Edmond, S. Wilcenski, J. Taylor. Mechanical and thermal properties of 3D-printed epoxy composites reinforced with boron nitride nanobarbs. *MRS Communications.* **2021**;11:100-105.
26. X. Xu, J. Yang, W. Jonhson, Y. Wang, A. Suwardi, J. Ding, C. Guan, D. Zhang. Additive manufacturing solidification methodologies for ink formulation. *Additive Manufacturing.* **2022**;56:102939.
27. E. Ayswarya, T. B. Sharmila, A. B. Nair, E. T. Thachil. Study On The Properties Of Epoxy-Wood Ash Composites: Mechanical Properties, Thermal Properties and Dynamic Mechanical Properties. *Materials Today: Proceedings.* **2023**;72:3100-3103.
28. J. Kathi, K.-Y. Rhee, J. H. Lee. Effect of chemical functionalization of multi-walled carbon nanotubes with 3-aminopropyltriethoxysilane on mechanical and morphological properties of epoxy nanocomposites. *Composites Part A: Applied Science and Manufacturing.* **2009**;40(6-7):800-809.
29. I. Raza, M. Hussain, A. N. Khan, T. Katzwinkel, J. Feldhusen. Properties of light weight multi walled carbon nano tubes (MWCNTs) nano-composites. *International Journal of Lightweight Materials and Manufacture.* **2021**;4(2):195-202.
30. N. S. Hmeidat, R. C. Pack, S. J. Talley, R. B. Moore, B. G. Compton. Mechanical anisotropy in polymer composites produced by material extrusion additive manufacturing. *Additive Manufacturing.* **2020**;34:101385.
31. M. Anas, M. M. Mustafa, A. Vashisth, E. Barnes, M. A. Saed, L. C. Moores, M. J. Green. Universal patterns of radio-frequency heating in nanomaterial-loaded structures. *Applied Materials Today.* **2021**;23:101044.
32. A. Vashisth, S. T. Upama, M. Anas, J.-H. Oh, N. Patil, M. J. Green. Radio frequency heating and material processing using carbon susceptors. *Nanoscale Advances.* **2021**;3(18):5255-5264.
33. M. Anas, Y. Zhao, M. A. Saed, K. J. Ziegler, M. J. Green. Radio frequency heating of metallic and semiconducting single-walled carbon nanotubes. *Nanoscale.* **2019**;11(19):9617-9625.
34. D. Debnath, X. Zhao, M. Anas, D. L. Kulhanek, J. H. Oh, M. J. Green. Radio frequency heating and reduction of graphene oxide and graphene oxide-polyvinyl alcohol composites. *Carbon.* **2020**;169:475-481.
35. N. Patil, X. Zhao, N. K. Mishra, M. A. Saed, M. Radovic, M. J. Green. Rapid heating of silicon carbide fibers under radio frequency fields and application in curing preceramic polymer composites. *ACS applied materials & interfaces.* **2019**;11(49):46132-46139.
36. C. B. Sweeney, A. G. Moran, J. T. Gruener, A. M. Strasser, M. J. Pospisil, M. A. Saed, M. J. Green. Radio frequency heating of carbon nanotube composite materials. *ACS applied materials & interfaces.* **2018**;10(32):27252-27259.
37. A. Sarmah, M. A. Morales, A. Srivastava, S. Upama, A. Nandi, T. C. Henry, M. J. Green, A. Vashisth. Interfacial carbon fiber–matrix interactions in thermosetting composites volumetrically cured by electromagnetic fields. *Composites Part A: Applied Science and Manufacturing.* **2023**;164:107276.

38. I. Enriquez, C. Noronha, K. Teo, A. Sarmah, S. Gupta, A. Nandi, B. Fishbeck, M. J. Green, A. Vashisth. Closed-Loop Composite Welding and Bonding System Using Radio-Frequency Heating and Pressure. *Journal of Composites Science.* **2023**;7(3):116.
39. S. S. Dasari, A. Sarmah, R. D. Mee, A. N. Khalfaoui, M. J. Green. Joule Heating of Carbon Fibers and Their Composites in Radio-Frequency Fields. *Advanced Engineering Materials.* **2023**:2201631.
40. A. Sarmah, S. K. Desai, G. B. Tezel, A. Vashisth, M. M. Mustafa, K. Arole, A. G. Crowley, M. J. Green. Rapid Manufacturing via Selective Radio-Frequency Heating and Curing of Thermosetting Resins. *Advanced Engineering Materials.* **2022**;24(7):2101351.
41. A. Sarmah, R. D. Mee, K. Arole, D. Chi, E. M. Harkin, S. S. Dasari, A. J. Wright, T. Q. Tran, A. Rout, M. J. Green. Competing Effects of Radio Frequency Fields on Carbon Nanotube/Resin Systems: Alignment versus Heating. *Macromolecular Materials and Engineering.* **2023**:2300174.
42. A. Sarmah, A. Crowley, S. Desai, G. Zolton, M. J. Green. ADDITIVE MANUFACTURING OF THERMOSETTING RESINS VIA DIRECT INK WRITING AND RADIO FREQUENCY HEATING AND CURING. In: US Patent App. 18/072,190; 2023.
43. P. Z. Ramos, A. Sarmah, M. J. Green, J. J. Richards. In situ investigation of the rheological and dielectric properties of a cross-linking carbon nanotube-thermosetting epoxy. *Soft Matter.* **2023**;19(32):6168-6175.
44. T. Q. Tran, A. Sarmah, E. M. Harkin, S. S. Dasari, K. Arole, M. J. Cupich, A. J. K. Wright, H. L. Seet, S. M. L. Nai, M. J. Green. Radio frequency-assisted curing of on-chip printed CNT/silicone heatsinks produced by material extrusion 3D printing. *Additive Manufacturing.* **2023**;78:103842.
45. Y. Wang, C. Cipriani, C.-M. Hsieh, H. Cao, A. Sarmah, K.-W. Liu, Z. Tan, M. J. Green, M. Radovic, P. Wei, E. B. Pentzer. Morphology map-guided identification of bijel ink for producing conductive porous structures. *Matter.* **2023**;6(11):4066-4085.
46. A. Sarmah, S. K. Desai, A. G. Crowley, G. C. Zolton, G. B. Tezel, E. M. Harkin, T. Q. Tran, K. Arole, M. J. Green. Additive manufacturing of nanotube-loaded thermosets via direct ink writing and radio-frequency heating and curing. *Carbon.* **2022**;200:307-316.

Footnotes

Abbreviations (include on the first page)

CNT – Carbon nanotubes, DIW – Direct ink write, RF – Radio frequency

Electrothermal free-form additive manufacturing of thermosets

Anubhav Sarmah[a,†], Ethan M. Harkin[a,†], Thang Q. Tran[a,b], Matthew J. Cupich[a], Micah J. Green[a,c]*

[a] Artie McFerrin Department of Chemical Engineering, Texas A&M University, College Station, TX, 77843, USA

[b] Singapore Institute of Manufacturing Technology (SIMTech), Agency for Science, Technology and Research (A*STAR), 2 Fusionopolis Way, Singapore 138634, Singapore

[c] Department of Materials Science & Engineering, Texas A&M University, College Station, TX, 77843, USA

[†:] These authors contributed equally to the work.

* Corresponding author: E-mail: micah.green@tamu.edu (Micah J. Green)

Supporting Information

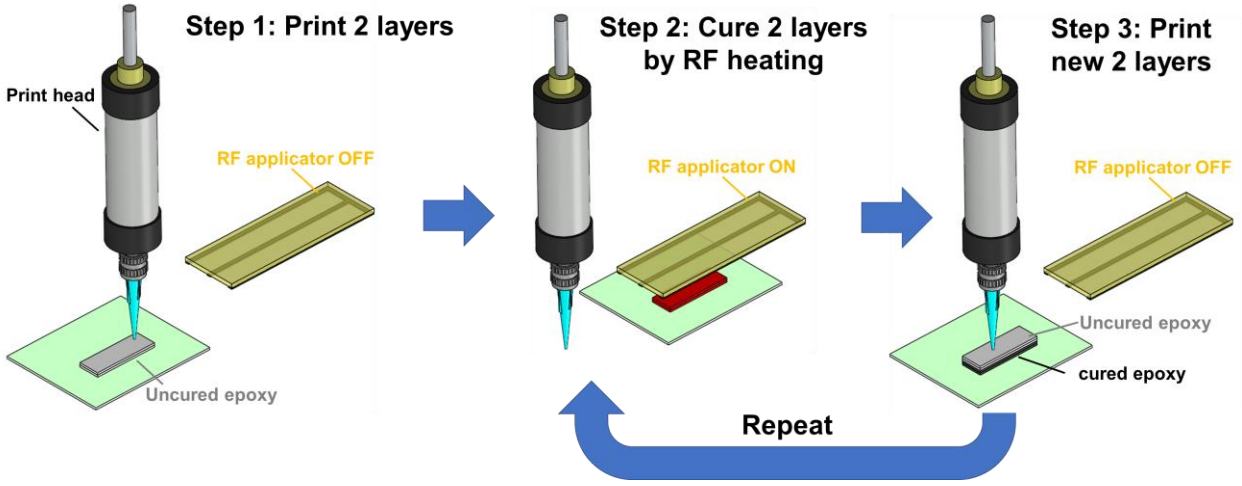

Figure S1: Schematic showing print-and-cure cycle for 3D printing of thermoset resins. After the first layer is printed, the part is exposed to RF fields from the top to induce heating and partial curing. Once sufficient cure is achieved, the print is resumed, and the process is repeated to print tall structures.

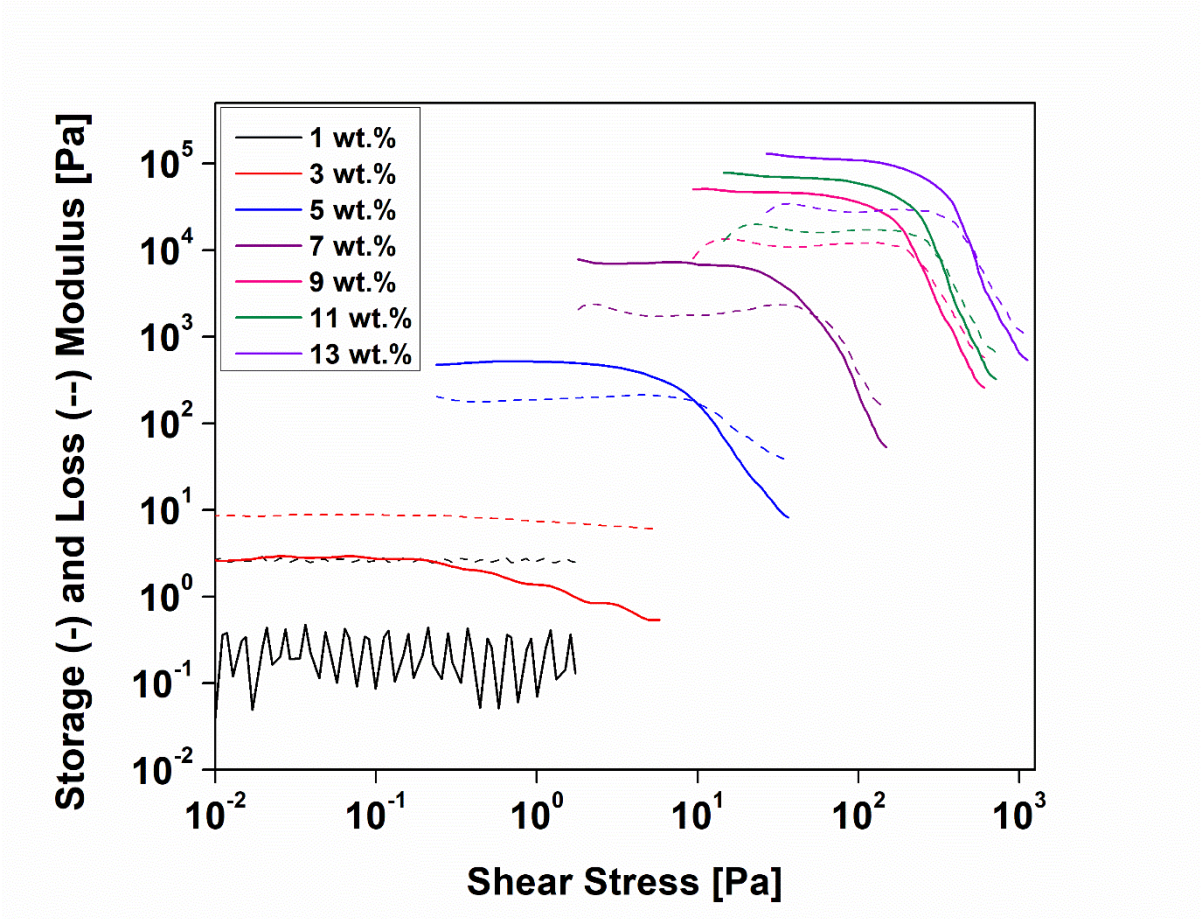

Figure S2: Storage and Loss modulus vs shear stress at room temperature for uncured resin at different CNT loadings.

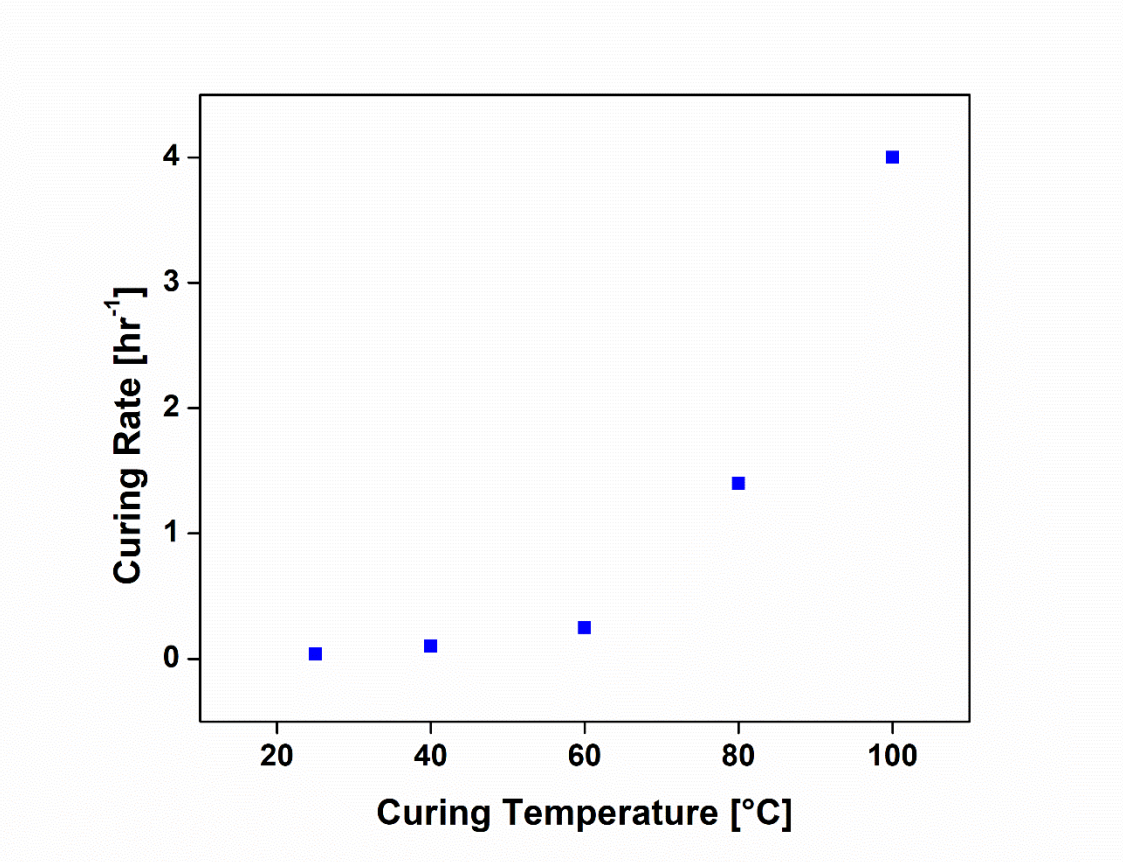

Figure S3: Curing rate (=1/Curing Time) measured using previously published rheological experiments for CNT-filled resin at different curing temperatures. Curing time (time required to reach ~95% cure) was evaluated by analyzing the evolution of storage modulus as a function of time.[1,2]

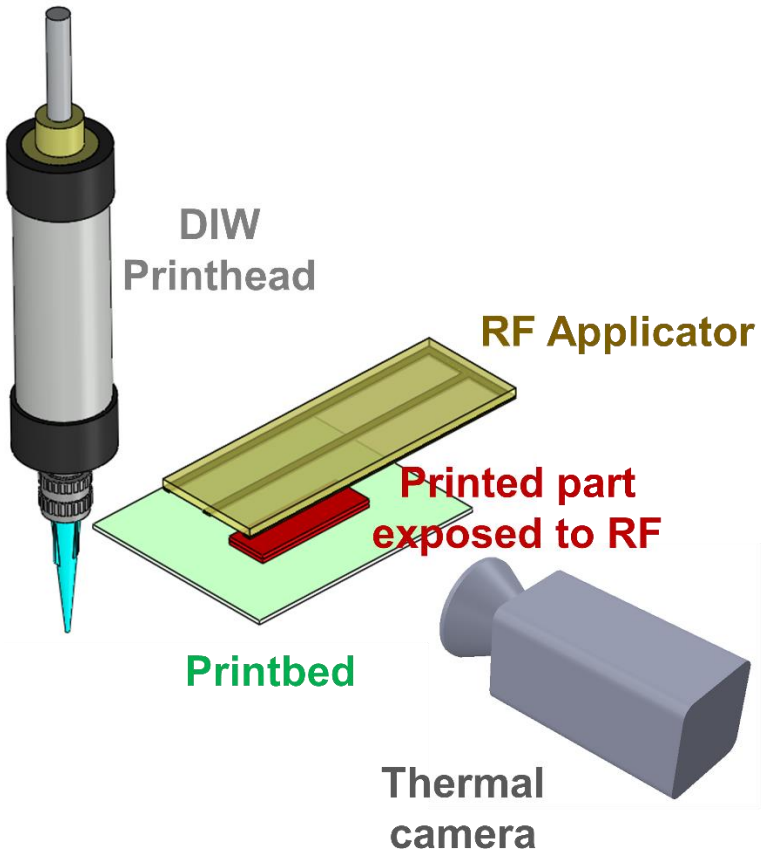

Figure S4: Experimental setup for RF-assisted DIW printing. A FLIR thermal camera monitors the maximum temperature of the sample when exposed to RF. This schematic is not to scale.

Table S1: Constants used for solving Equation 2.[1]

$$\frac{d\alpha}{dt} = (k\alpha^m)(1-\alpha)^n$$

Parameter (Symbol)	Value/Expression
Activation Energy (E_a)	33 kJ/mol
Reference temperature (T_{ref})	80 °C
Rate constant at reference temperature (k_{ref})	0.00276 s^{-1}
Gas constant (R)	8.314 J/(mol-K)
Temperature (T)-dependent rate constant (k)	$k_{ref}e^{-\frac{E}{R}(\frac{1}{T}-\frac{1}{T_{ref}})}$ [s^{-1}]
m	0.352
n	1

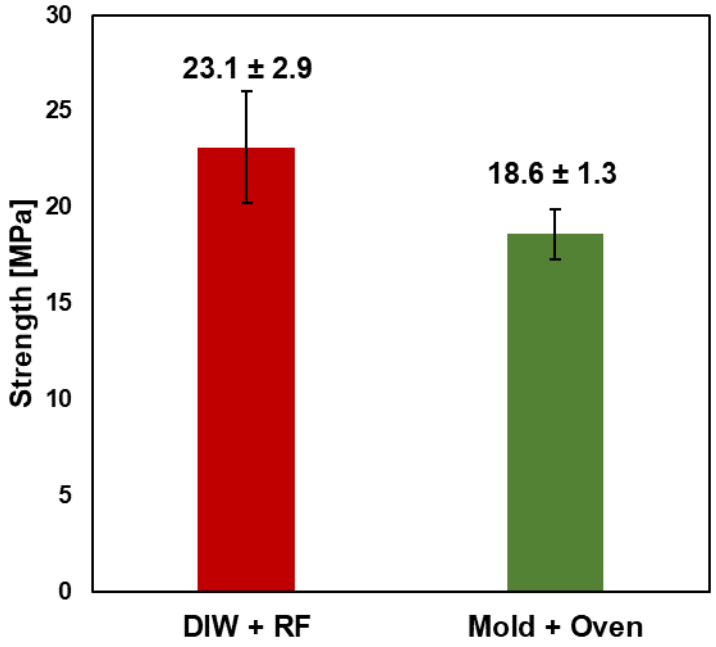

Figure S5: Ultimate tensile strength values for 4 wt.% epoxy-CNT composite, ASTM D638 Type IV tensile bars cured using DIW Printing + RF heating and oven curing in a mold. Reproduced from our prior work.[3]

References

1. G. B. Tezel, A. Sarmah, S. Desai, A. Vashisth, M. J. Green. Kinetics of carbon nanotube-loaded epoxy curing: Rheometry, differential scanning calorimetry, and radio frequency heating. *Carbon.* **2021**;175:1-10.
2. P. Z. Ramos, A. Sarmah, M. J. Green, J. J. Richards. In situ investigation of the rheological and dielectric properties of a cross-linking carbon nanotube-thermosetting epoxy. *Soft Matter.* **2023**;19(32):6168-6175.
3. A. Sarmah, S. K. Desai, A. G. Crowley, G. C. Zolton, G. B. Tezel, E. M. Harkin, T. Q. Tran, K. Arole, M. J. Green. Additive manufacturing of nanotube-loaded thermosets via direct ink writing and radio-frequency heating and curing. *Carbon.* **2022**;200:307-316.